Reconciling the electron counterstreaming and dropout occurrence rates with the heliospheric flux budget

Article

Published Version

JOURNAL OF GEOPHYSICAL RESEARCH, VOL. 112, A06106, doi:10.1029/2006JA012159, 2007

Reconciling the electron counterstreaming and dropout occurrence rates with the heliospheric flux budget

M. J. Owens[1] and N. U. Crooker[1]

Received 4 November 2006; revised 29 January 2007; accepted 8 February 2007; published 5 June 2007.

[1] Counterstreaming electrons (CSEs) are treated as signatures of closed magnetic flux, i.e., loops connected to the Sun at both ends. However, CSEs at 1 AU likely fade as the apex of a closed loop passes beyond some distance R, owing to scattering of the sunward beam along its continually increasing path length. The remaining antisunward beam at 1 AU would then give a false signature of open flux. Subsequent opening of a loop at the Sun by interchange reconnection with an open field line would produce an electron dropout (ED) at 1 AU, as if two open field lines were reconnecting to completely disconnect from the Sun. Thus EDs can be signatures of interchange reconnection as well as the commonly attributed disconnection. We incorporate CSE fadeout into a model that matches time-varying closed flux from interplanetary coronal mass ejections (ICMEs) to the solar cycle variation in heliospheric flux. Using the observed occurrence rate of CSEs at solar maximum, the model estimates $R \sim 8-10$ AU. Hence we demonstrate that EDs should be much rarer than CSEs at 1 AU, as EDs can only be detected when the juncture points of reconnected field lines lie sunward of the detector, whereas CSEs continue to be detected in the legs of all loops that have expanded beyond the detector, out to R. We also demonstrate that if closed flux added to the heliosphere by ICMEs is instead balanced by disconnection elsewhere, then ED occurrence at 1 AU would still be rare, contrary to earlier expectations.

Citation: Owens, M. J., and N. U. Crooker (2007), Reconciling the electron counterstreaming and dropout occurrence rates with the heliospheric flux budget, *J. Geophys. Res.*, *112*, A06106, doi:10.1029/2006JA012159.

1. Introduction

[2] Suprathermal electrons have long been used as tracers of the topology of the heliospheric magnetic field (HMF), with a single field-aligned beam (or "strahl") being indicative of open magnetic flux and counterstreaming electron (CSE) beams signifying flux with both foot points rooted at the Sun (the energization of electrons far from the Sun, such as at corotating shocks and planetary sources, is likely to produce a negligible contribution to the total CSE rate observed at 1 AU [e.g., *Wimmer-Schweingruber et al.*, 2006, and references therein]). The closed flux topologies indicated by CSEs are strongly associated with interplanetary coronal mass ejections (ICMEs) [*Gosling et al.*, 1987]. Periods when no field-aligned suprathermal electron beams are observed, termed "heat flux dropouts" (HFDs), were initially thought to be signatures of reconnection between open field lines resulting in flux completely disconnected from the Sun (see also the bottom panels of Figure 1 [*McComas et al.*, 1989]). *McComas et al.* [1989] argued that disconnection must be the means of balancing the closed flux introduced to the heliosphere from CMEs. A balance is required to avoid any buildup over the solar cycle. They also noted, however, that the scarcity of HFDs observed in the solar wind at 1 AU seemed inconsistent with this view. Following *Gosling et al.* [1995], *Crooker et al.* [2002] pointed out that there is no inconsistency if ICME fields open via "interchange reconnection" between the legs of the closed loops and open fields close to the Sun (illustrated in the top panels of Figure 1), in which case no disconnection is required.

[3] *Owens and Crooker* [2006] (hereafter "Paper 1") expanded on the ideas of *Crooker et al.* [2002] to show that if the closed fields in ICMEs open slowly (over many tens of days), their flux contribution is sufficient to explain the solar cycle doubling in HMF intensity observed at 1 AU. They developed a quantitative model of the heliospheric flux consisting of two components: constant open flux from large-scale coronal holes and time-varying closed flux accumulated from CMEs. Here we further develop the model so as to predict suprathermal electron signatures of heliospheric flux buildup from long-lived ICME closed flux. We demonstrate how HFDs can result from interchange reconnection as well as disconnection, and we conclude that the HFD occurrence rate at 1 AU for either process should be much lower than the occurrence rate of CSEs, in agreement with observations.

[1]Center for Space Physics, Boston University, Boston, Massachusetts, USA.

0148-0227/07/2006JA012159$09.00

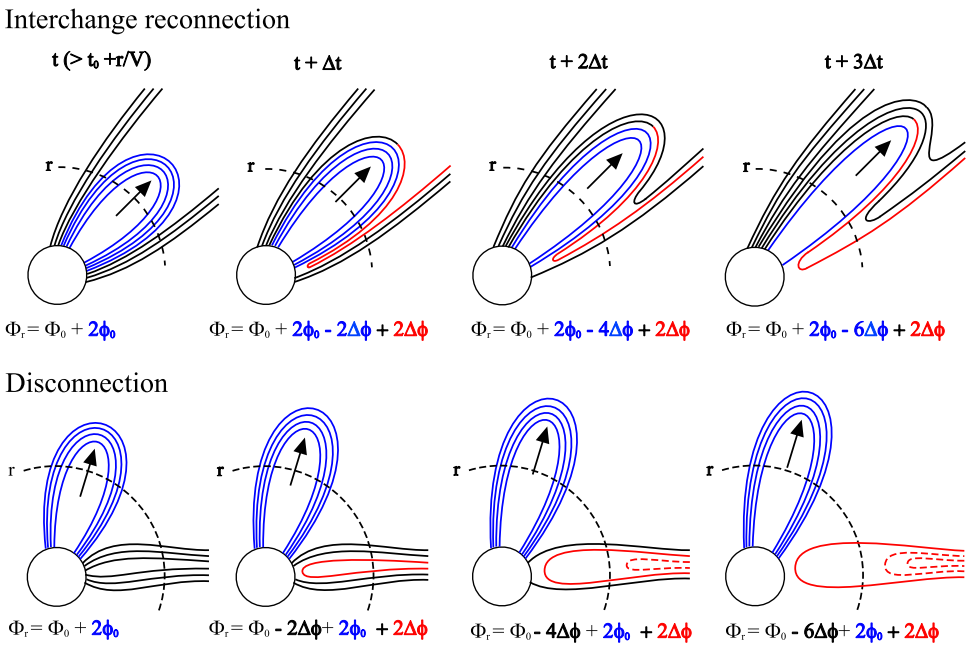

Figure 1. A sketch of the various flux systems that contribute to the total heliospheric flux at a distance r (Φ_r). Each line represents a flux tube containing flux $\Delta\phi$. The top panels show interchange reconnection: The total open flux contribution (Φ_0, shown as black lines) is constant with time. Blue lines indicate closed flux: Initially the CME contributes $2\phi_0$ (where ϕ_0 is the total posteruption axial flux), as each flux tube intersects the sphere of radius r twice. In a time Δt, $\Delta\phi$ of this closed flux will open via interchange reconnection close to the Sun, or $\Delta\phi$ of open flux will disconnect. There is also a contribution to Φ_r from "inverted" flux for interchange reconnection, shown as red lines: This is the result of newly reconnected field lines yet to propagate to r. The bottom panels show disconnection: The injected closed flux is balanced by a reduction in the open flux. Solid red lines show the disconnected flux yet to propagate to r.

[4] Throughout the rest of this paper, we use the more specific "electron dropout" (ED) in place of HFD to designate a drop in total electron number density in the suprathermal energy range, since heat flux can drop through a redistribution in pitch angle as well as through disconnection [e.g., *Pagel et al.*, 2005].

2. Heliospheric Flux From CMEs

[5] To calculate the expected suprathermal electron signatures of long-lived ICME closed flux, we must adapt the model of heliospheric flux outlined in Paper 1 to account for the effects of nonzero propagation time of both the ICME closed loops and newly opened flux. Figure 1 shows an overview of two possible types of heliospheric flux evolution: The top panels show how flux added by ICMEs is removed by opening the ICME flux via interchange reconnection, and the bottom panels show how the ICME-added flux can be balanced by disconnecting the same amount of open flux. Each line represents a flux tube containing flux $\Delta\phi$. We first consider the interchange reconnection scenario. The open flux (black lines) contributes Φ_0 (=6$\Delta\phi$ as shown in the figure) to the total flux threading a sphere at a heliocentric distance r, denoted Φ_r. Although the topology of open flux changes with the evolving ICME flux, Φ_0 remains constant with time.

[6] At time t_0, the CME erupts and carries a posteruption axial flux of ϕ_0 (=4$\Delta\phi$ as shown in the figure), where $\phi_0 = (1 - D)\phi_A$, D being the fraction of flux that opens during CME formation and ϕ_A the total axial flux content of the CME. This new flux system can only contribute to Φ_r once the loops reach r, i.e., when $t \geq t_0 + v/r$, where v is the transit speed of the ICME. (We do not consider the time required for an ICME to move past an observer at r, which depends upon both the ICME radial width and expansion speed.) The closed flux contribution (blue lines) Φ_C at $t \geq t_0 + r/v$ is $2\phi_0$, since each flux tube intersects the sphere of radius r twice, minus any opened flux. Newly opened ICME flux (red lines) takes a time r/v to propagate to r, during which it will continue to contribute to Φ_r as if it were closed. We refer to this flux system as the "inverted flux" Φ_I.

[7] For disconnection, in contrast to interchange reconnection, the closed flux contribution of a CME ϕ is constant. The open flux contribution decays at the exact same rate at which ICME flux opens in the interchange reconnection scenario, since the same amount of flux added to the heliosphere by CMEs must be removed over the solar cycle. Consequently, the instantaneous value of Φ_r is the same for disconnection and interchange reconnection, but the contributing flux systems are different, as shown Figure 1. The disconnected flux contribution (Φ_D, solid red lines) to Φ_r is equal to the inverted flux contribution Φ_I.

[8] Thus Φ_r, the flux threading a heliocentric sphere of radius r, can be considered to consist of three components:

[9] Interchange reconnection:

$$\Phi_r = \Phi_0 + \Phi_C + \Phi_I = \Phi_0 + 2\left(\phi_0 - \int_{t_0}^{t} \frac{\partial \phi_C}{\partial t} dt\right) + 2\left(\int_{t-r/v}^{t} \frac{\partial \phi_C}{\partial t} dt\right)$$

[10] Disconnection:

$$\Phi_r = \Phi_0 + \Phi_C + \Phi_D = \left(\Phi_0 - 2\int_{t_0}^{t} \frac{\partial \Phi_0}{\partial t} dt\right) + 2\phi_0 + 2\left(\int_{t-r/v}^{t} \frac{\partial \Phi_0}{\partial t} dt\right) \quad (1)$$

where ϕ_C is the instantaneous ICME closed flux. The rate of reconnection, involving either open flux disconnection or closed ICME flux opening, is determined by the heliospheric flux budget and must therefore be equal. As in Paper 1, we consider two forms for the reconnection rate: (1) a constant k and (2) proportional to the amount of closed flux. Thus for $t \leq t_0 + \phi/k$:

[11] (1) Constant reconnection rate:

$$\left[\frac{\partial \Phi_0}{\partial t}\right]_{Disc.} = \left[\frac{\partial \phi_C}{\partial t}\right]_{Int.rec.} = -k$$

[12] (2) Reconnection rate proportional to ϕ:

$$\left[\frac{\partial \Phi_0}{\partial t}\right]_{Disc.} = \left[\frac{\partial \phi_C}{\partial t}\right]_{Int.rec.} = -\lambda\phi_C = -\lambda\phi_0 \exp[-\lambda(t - t_0)] \quad (2)$$

For $t > t_0 + \phi/k$, all the closed flux has opened in the constant flux-opening rate model, and thus k becomes zero.

[13] Combining equations (1) and (2) yields the same equations for Φ_r for both disconnection and interchange reconnection:

[14] (1) Constant reconnection rate:

$$\Phi_r = \Phi_0 + 2[\phi_0 - k(t - t_0)] + 2kr/v$$

[15] (2) Reconnection rate proportional to ϕ:

$$\Phi_r = \Phi_0 + 2\phi_0 \exp[-\lambda(t - t_0)] + 2\phi_0 \exp[-\lambda(t - t_0)]\left(\exp\left[\frac{r\lambda}{v}\right] - 1\right) \quad (3)$$

[16] The black lines in Figure 2 show the total flux contribution of a single ICME to a sphere of radius r = 1 AU (i.e., Φ_{1AU}) as a function of time past the CME eruption time. Solid (dashed) lines show the exponential (constant) flux-opening model. The top-left panel gives results for ICME opening via interchange reconnection. There is no contribution to Φ_{1AU} until ~3–4 days, when the leading edge of the ICME reaches 1 AU. (An ICME transit speed of 450 km/s is assumed.) The blue and red lines show the contributions from closed and inverted flux, respectively.

[17] The bottom-left panel of Figure 2 gives results for disconnection. The increase in heliospheric flux at r is shown by the black lines and is identical to that of interchange reconnection. The closed flux contribution (blue lines) is constant, but the overall flux decreases because of a decrease in the open flux (not shown).

[18] To estimate the total ICME contribution to the heliospheric flux, it is necessary to sum over all ICMEs in the heliosphere that have both propagated to r and that still contain some closed flux. Assuming there are N such ejecta at time t, the total flux for both disconnection and interchange reconnection is given by:

[19] (1) Constant reconnection rate:

$$\Phi_r(t) = \Phi_0 + \sum_{n=1}^{N} 2\left[\phi_0^n - k^n\left(t - t_0^n\right)\right] + \sum_{n=1}^{N} 2k^n r/v^n$$

[20] (2) Reconnection rate proportional to ϕ:

$$\Phi_r(t) = \Phi_0 + \sum_{n=1}^{N} 2\phi_0^n \exp\left[-\lambda^n\left(t - t_0^n\right)\right] + \sum_{n=1}^{N} 2\phi_0^n \exp\left[-\lambda^n\left(t - t_0^n\right)\right]\left(\exp\left[\frac{r\lambda^n}{v^n}\right] - 1\right) \quad (4)$$

where the superscript n is used to index the ICMEs (and their properties) in the heliosphere.

3. Implications for Electron Observations

[21] In this section we consider the implications of interchange reconnection and disconnection on observable in situ electron signatures. Figure 3 shows the suprathermal electron strahl direction (red arrows) along magnetic field lines (black lines) for various heliospheric flux systems. The top two sets of panels show ICME flux opening by interchange reconnection. In a "fast" ICME flux-opening scenario (Figure 3a), closed loops always exhibit a CSE signature, whereas open field lines (including the inverted flux) always exhibit a single strahl. For the "slow" ICME flux-opening scenario (Figure 3b), we consider the consequences of suprathermal electron scattering. The blue shaded region shows the heliocentric distance beyond which we assume that sunward electron beams can no longer reach the observing site, having scattered in some unspecified way along the long path from the far foot point. For clarity, the substantial increase in field-line length owing to solar rotation (illustrated in Figure 6) has been ignored here. If ICMEs remain closed for long periods, their CSE signatures will fade when their leading edges reach such distances. When interchange reconnection eventually opens the ICME flux, the remaining antisunward electron beam will be cut off, leaving the inverted flux devoid of suprathermal electrons. This electron dropout was originally thought to signify only flux completely disconnected from the Sun [*McComas et al.* [1989], as discussed below]. In our interpretation, EDs could also be signatures of ICME closed loops opening over very long timescales.

[22] Thus for $t \geq t_0 + R/v$, where R is the distance from the Sun where the field lines are sufficiently long that the sunward electron strahl scatters, the signature of closed flux switches from a CSE signature to a single antisunward strahl (and thus is indistinguishable from open flux), and the signature of inverted flux switches from a sunward single

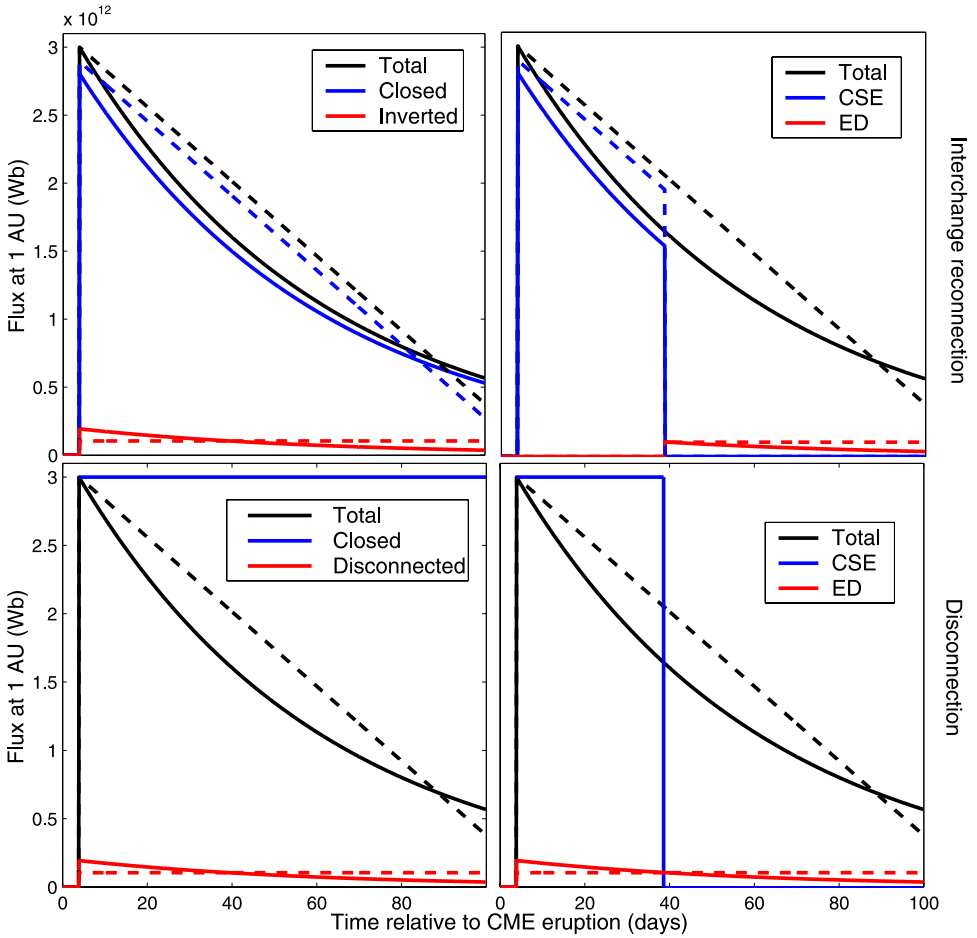

Figure 2. Flux contribution from a single ICME to the total flux threading a heliocentric sphere of radius 1 AU (Φ_{1AU}) as a function of time past CME launch. The top (bottom) two panels show ICME fields opening via interchange reconnection (being balanced by open flux disconnection). Solid (dashed) lines show the exponential (constant) flux-opening model. The left panels show the total contribution of the ICME to Φ_{1AU} (black lines), along with the individual contributions from closed (blue) and inverted/disconnected (red) flux systems. The right panel again shows the total contribution of a single CME to Φ_{1AU} (black lines), but with the fraction of that flux exhibiting counterstreaming electrons (blue) and electron dropouts (red), assuming suprathermal electrons scatter when the leading edge of the CME reaches 10 AU. See also Figure 3.

strahl to an ED. The signature of true open flux remains unchanged as a single strahl throughout this process. The top-right panel of Figure 2 shows the total flux contribution to Φ_r from an ICME as a function of time past CME eruption (black dashed lines), and the fractions of that flux displaying CSEs (red) and EDs (blue), assuming the suprathermal electron strahl scatters at a distance R = 10 AU.

[23] Despite disconnection and interchange reconnection producing the same values for the magnitude of the heliospheric magnetic flux, they may produce different suprathermal electron signatures: Disconnection involves destruction and creation of open flux, which are topologically different from the conservation of open flux that occurs with interchange reconnection. The bottom-right panel of Figure 2 shows the electron signatures for disconnection, with red lines showing EDs resulting from true disconnection. Unlike interchange reconnection, these ED signatures are present both before and after the ICME leading edge reaches the suprathermal electron fadeout distance. The closed field contribution will display CSEs until the ICME leading edge reaches R (blue lines).

[24] In the following sections we use these heliospheric flux models to quantitatively estimate how frequently CSE and ED signatures should be observed at 1 AU.

4. Static Equilibrium

[25] As in Paper 1, it is instructive first to investigate a static equilibrium wherein CMEs are injected into the heliosphere at a constant frequency f. Thus Δt, the time between consecutive CMEs, is simply $1/f$.

[26] At a time t, the last ICME contributing to Φ_r (i.e., the Nth ICME) is the last ejection to reach just to the height of observation (r). Hence $N = 1 + (t - r/v)/\Delta t$. The injection time of the nth CME is then given by:

$$t_0^n = t_0^N - \frac{r}{v} - \Delta t(N - n) = \frac{n - 1}{f} \quad (5)$$

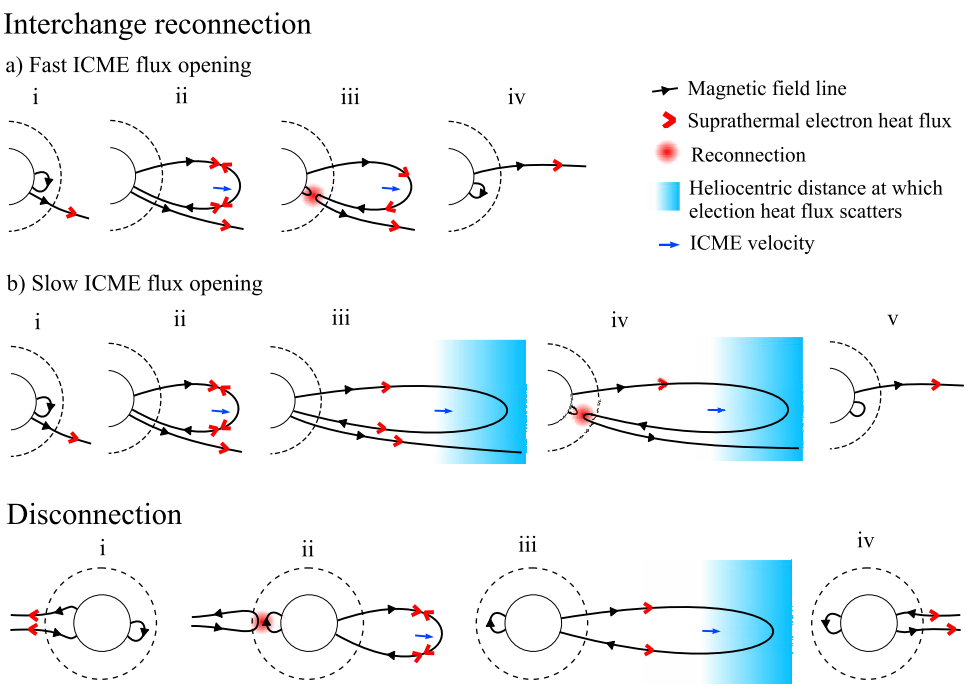

Figure 3. Suprathermal electron signatures of heliospheric flux buildup. Magnetic field lines are shown as solid black lines/arrows and electron beams by red arrows. The dashed line represents a surface at the heliocentric distance at which flux is observed. The top two panels show interchange reconnection: In the case of (a) "fast" ICME flux-opening, closed flux is identifiable by a counterstreaming electron (CSE) signature, which is removed once interchange reconnection opens the loop. However, for (b) "slow" flux-opening, it is necessary to consider the effect of suprathermal electron scattering due to the length of field lines. This can result in no CSE signature on closed loops, and electron dropouts on inverted flux systems. The bottom panel shows ICME flux balanced by disconnection of open flux, which immediately results in ED signatures.

For the constant reconnection rate mode, there is a limit to the number of ICMEs that can contribute to the heliospheric flux: For the interchange reconnection scenario, an ICME has no closed flux after a time $t_C = \phi_0/k$ and will not contribute to the inverted flux after a time $t_F = \phi_0/k + r/v$. Thus the earliest ICME that can still contribute to the closed (inverted) flux system is $n = f[t - t_C]$ ($n = f[t - t_F]$), rounded up to the nearest positive integer.

[27] Assuming all CMEs have the same properties (i.e., ϕ_0^n, λ^n, and v^n can be represented by average values ϕ_0, λ, and v, respectively), we express the flux at r resulting from both disconnection and interchange reconnection as:

[28] (1) Constant reconnection rate:

$$\Phi_r(t) = \Phi_0 + \sum_{n=f(t-t_C)}^{N} 2\left[\Phi_0 - k\left(t - \frac{n-1}{f}\right)\right] + \sum_{n=f(t-t_F)}^{N} 2\frac{kr}{v}$$

$$= \Phi_0 + \sum_{n=1}^{1+f(t_C-r/v)} 2\left[\phi_0 - k\left(t_C - \frac{n-1}{f}\right)\right] + \sum_{n=1}^{1+ft_C} 2\frac{kr}{v}$$

[29] (2) Reconnection rate proportional to ϕ:

$$\Phi_r(t) = \Phi_0 + \sum_{n=1}^{N} 2\phi_0 \exp\left[-\lambda\left(t - \frac{n-1}{f}\right)\right] + \sum_{n=1}^{N} 2\phi_0 \exp\left[-\lambda\left(t - \frac{n-1}{f}\right)\right]\left(\exp\left[\frac{r\lambda}{v}\right] - 1\right) \quad (6)$$

[30] As an equilibrium is attained (i.e., as $t \to \infty$), these expressions simplify to:

[31] (1) Constant reconnection rate:

$$\Phi_r(t) = \Phi_0 + \phi_0\left(1 + \frac{f\phi_0}{k}\right) + \frac{kfr^2 + krv}{v^2}$$

[32] (2) Reconnection rate proportional to ϕ:

$$\Phi_r(t) = \Phi_0 + \frac{2\phi_0}{1 - \exp[\lambda/f]} \quad (7)$$

[33] By considering solar minimum and maximum conditions separately (see Table 1 and Paper 1), and assuming radial flux is constant over the heliocentric sphere (i.e., $\Phi_r = 4\pi r^2|B_{\mathrm{RAD}}|$, where $|B_{\mathrm{RAD}}|$ is the radial magnetic field strength at r), we find the following: (1) k = 1.4 Wb/day, which translates to half the posteruption flux opening (or the equivalent open flux disconnecting) in 55 days, and Φ_0 = 9.3 $\times$ 10^{14} Wb, and (2) λ = 2.1 $\times$ 10^{-7} days, which translates to a closed flux half-life (or timescale for disconnection of open flux) of ~38 days, and Φ_0 = 9.4 $\times$ 10^{14} Wb. These estimates of the reconnection rates are the same as in Paper 1 because the additional inverted/disconnected flux contributions are negligible. This implies that EDs should only comprise a tiny fraction of the total flux, since in the interchange reconnection (disconnection) scenario, EDs can only be produced on this inverted (disconnected) flux system.

Table 1. Observational Estimates for the Parameters of the Heliospheric Flux Budget Calculation

Parameter	Symbol	Value
Average Solar Maximum $\|\mathbf{B}\|$ at 1 AU	$\|\mathbf{B}_{MAX}\|$	8 nT
Average Solar Minimum $\|\mathbf{B}\|$ at 1 AU	$\|\mathbf{B}_{MIN}\|$	5 nT
Average Solar Maximum CME Rate	f_{MAX}	4 day^{-1}
Average Solar Minimum CME Rate	f_{MIN}	1/3 day^{-1}
Typical Axial Flux in an ICME	ϕ_A	3×10^{12} Wb
Typical Fraction of ϕ that Opens at Formation	D	0.5

[34] As in Paper 1, we note that because the axial flux of magnetic clouds is being used as the value for all CMEs, ϕ is probably being overestimated. Hence the derived ICME flux-opening (open flux disconnection) times are best regarded as lower limits. On the other hand, Figure 2 shows that even for a constant (exponential) reconnection half-life as low as 55 (38) days, around a sixth (third) of the CME posteruption flux, which is a 12th (sixth) of the total axial flux, still remains closed after 100 days.

[35] Figure 4 shows the percentage flux at 1 AU expected to exhibit CSE (blue) and ED (red) signatures for CME frequencies at solar minimum (left panel) and solar maximum (right panel) over a range of values for R (the ICME distance beyond which the sunward suprathermal electron strahl at 1 AU fades out). Dashed (solid) lines show constant (exponential) reconnection times with a half-life of (55) 38 days and a background open flux of 9.3×10^{14} (9.4×10^{14}) Wb. The percentage of total flux displaying CSE and ED signatures in Figure 4 directly translates to the percentage of time CSE and ED signatures are expected at 1 AU (i.e., the rate of occurrence). The top panels show the results for interchange reconnection: Our model of heliospheric flux evolution with best observation estimates for the required parameters predicts that ED signatures should be rare (i.e., limited to $\leq$5%), even at solar maximum. CSE signatures are predicted to show a strong solar cycle variation, although the exact numbers depend strongly on the distance at which the strahl scatters.

[36] Ulysses observations have shown that CSEs persist to at least to 5 AU [*Crooker et al.*, 2004; *Riley et al.*, 2004],

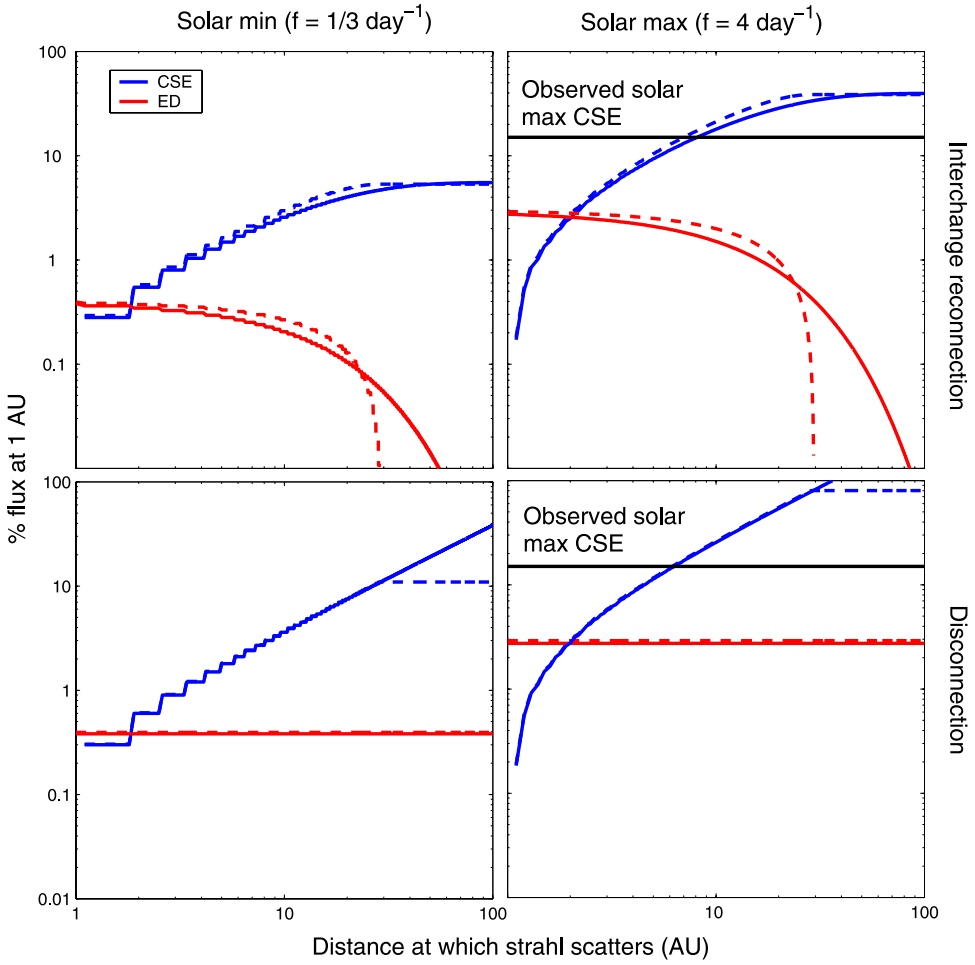

Figure 4. Predicted percentages of CSE (blue) and ED (red) signatures for CME frequencies at solar minimum (left) and maximum (right) at 1 AU, for a range of R, the distance at which the suprathermal electron strahl scatters. Top (bottom) panels show the interchange reconnection (disconnection) methods of reducing heliospheric flux. Dashed (solid) lines show constant (exponential) ICME flux opening with a half-life of (55) 38 days and a background open flux of 9.3×10^{14} (9.4×10^{14}) Wb is used. Note the logarithmic scale on both axes.

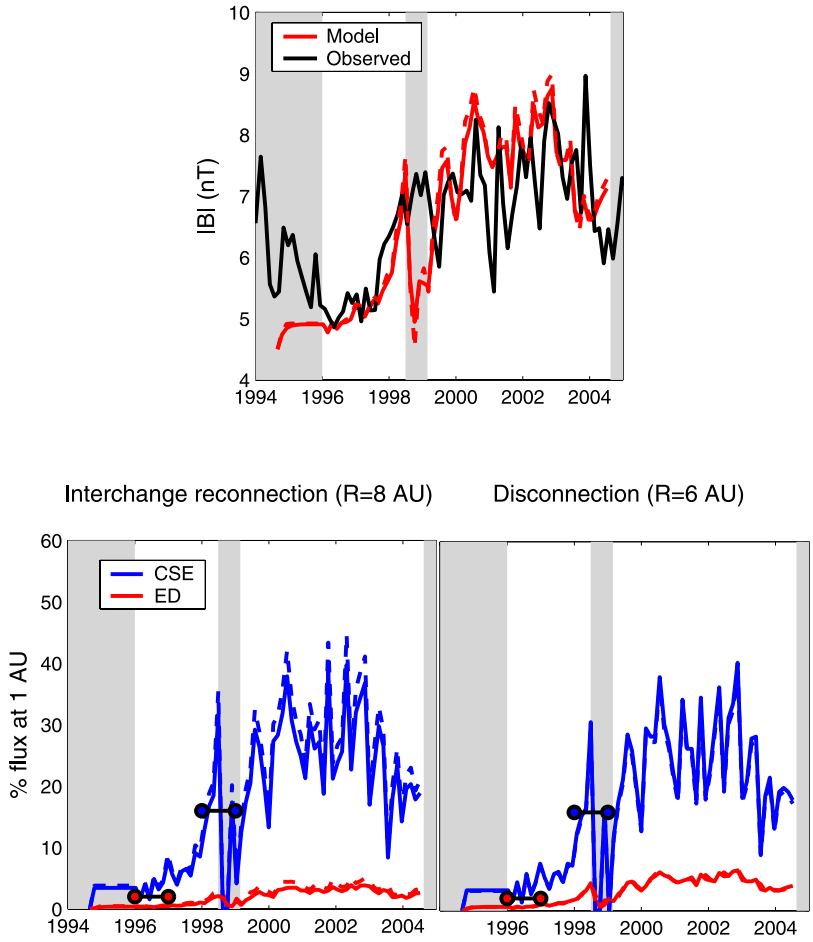

Figure 5. Magnetic flux and suprathermal electron signatures for simulations driven with LASCO-observed CME eruption times. Gray-shaded regions are times when LASCO observations were unavailable. Solid (dashed) lines show the exponential (constant) flux-opening model with a half-life of 38 (55) days. The top panel shows the model-predicted (red) and observed (black) magnetic field intensity at 1 AU: As in Paper 1, a good agreement is found. The bottom-left (bottom-right) panel shows the model-predicted occurrence of CSE and ED signatures at 1 AU for the interchange reconnection (disconnection) process, assuming the strahl scatters at 8 AU (6 AU). Observed occurrence rates of CSEs (EDs) are shown as black lines with blue (red) circles.

which means that a lower bound of 5 AU can be placed on R. This limits the predicted occurrence rate of CSEs to ~1–6% at solar minimum, rising to ~8–40% at solar maximum. *Gosling et al.* [1992] examined the ISEE 3 electron data and observed counterstreaming 15% of the time near maximum of solar cycle 22. From this value we obtain an estimate for R of 8 AU, as indicated by where the black line intersects the blue curves in the top-right panel of Figure 4.

[37] The bottom panels of Figure 4 show the equivalent results for disconnection: Contrary to *McComas et al.* [1992], we find that disconnection should not produce an abundance of ED signatures at 1 AU. However, the disconnection scenario produces more CSE signatures than the interchange reconnection scenario, with the observations of *Gosling et al.* [1992] best matched by R = 6 AU.

5. Dynamic Simulations

[38] In this section, the models are driven using the CME eruption times listed in the LASCO CME catalogue [*Yashiro et al.*, 2004], following an initiation period with a constant rate of 0.5 day^{-1}. At each time step, equation (4) is solved. Figure 5 shows the simulated magnetic flux and suprathermal electron signatures at 1 AU. Gray panels show times when LASCO observations were unavailable. Solid (dashed) lines show the exponential (constant) reconnection model with a half-life of 38 (55) days. The red plots in the top panel show the model-predicted magnetic field intensities at 1 AU, while the black line shows the observed value taken from the National Space Science Center (OMNI) data, averaged over 50 days (this long timescale is required for the observed magnetic field strength to be representative of the heliospheric flux [*Lockwood et al.*, 2004]). As in Paper 1, we find good agreement with the overall solar cycle variation of $|\mathbf{B}|$ at 1 AU.

[39] The bottom-left (bottom-right) panel of Figure 5 shows the model-predicted occurrence of CSE and ED signatures at 1 AU for the interchange reconnection (disconnection) process, assuming the strahl scatters at 8 AU (6 AU). It is immediately obvious that interchange reconnection and

disconnection can produce very similar electron signatures at 1 AU, although different values of R were used. Since here we do not model the latitudinal confinement of CME signatures at solar minimum, the CSE and ED signatures are probably underestimated at this time. At solar maximum, the occurrence of CSEs is highly variable, with a mean value of ~25%, slightly higher than *Gosling et al.*'s [1992] estimate for the previous cycle. At minimum of cycle 22, *Gosling et al.* [1992] found very few periods with CSE signatures (~1%), although the total data coverage at that time was poor (20%). This is also lower than the model prediction for cycle 23. Using data from the ACE spacecraft, *Skoug et al.* [2000] reported a slightly higher occurrence rate for CSEs of ~16% on the rise to the maximum of cycle 23 (shown as black line with blue circles in Figure 5), in close agreement with the model. For both interchange reconnection and disconnection, the occurrence of EDs remains below the 5–7% level throughout the simulation, which is roughly a factor 4–5 lower than the CSE occurrence rate. These low ED percentages suggest consistency with their perceived rarity in the heliosphere [*Pagel et al.*, 2005]. What is new is the model demonstration that this rarity does not imply an imbalance in the heliospheric flux budget. Thus the available suprathermal electron observations for the modeled solar cycle are in general agreement with the model of heliospheric flux evolution via interchange reconnection with $R \sim 8$ AU and via disconnection with $R \sim 6$ AU.

6. Discussion

[40] We have extended the heliospheric flux model of *Owens and Crooker* [2006] to predict the suprathermal electron signatures of heliospheric flux buildup from coronal mass ejections. We assume that either the closed fields of the ejecta open via interchange reconnection or disconnection occurs elsewhere: Both methods produce similar electron signatures at 1 AU. We find that the distance R beyond which suprathermal electrons fail to return to the observing point as sunward counterstreaming beams on closed loops owing to scattering is a critical parameter in determining the predicted occurrence rate of counterstreaming electrons and electron dropouts at 1 AU. Indeed, R may provide a means to differentiate between interchange reconnection and disconnection. CSE observations are best matched when $R \sim 8$ AU for interchange reconnection and when $R \sim 6$ AU for disconnection. The former seems to be the more reasonable value since counterstreaming is commonly observed at 5 AU [e.g., *Crooker et al.*, 2004]. The spiral nature of the field lines means that these R values are equivalent to a scattering distance ~30–40 AU, as illustrated in Figure 6.

[41] Our model assumes only that the sunward suprathermal electron strahl scatters once field lines reach a certain length. Adiabatic effects must also play a role. Figure 6 shows an ICME field line when the leading edge of the ejecta is at 8 AU. Suprathermal electrons must travel ~40 AU to provide the counterstreaming signature at 1 AU. Note that the antisunward (sunward) traveling electrons are moving into weaker (stronger) magnetic fields and therefore will be adiabatically focused (defocused). However, rather than focussing with distance from the Sun, electron beams are observed to broaden owing to scattering [*Hammond et al.*, 1996; *Maksimovic et al.*, 2005]. An adiabatic sunward return of these broadened strahls will then further defocus them. Hence a field line may exhibit CSEs at 8 AU but only a single strahl at 1 AU. This effect implies a slight overprediction of CSE and underprediction of ED occurrence rates over the solar cycle.

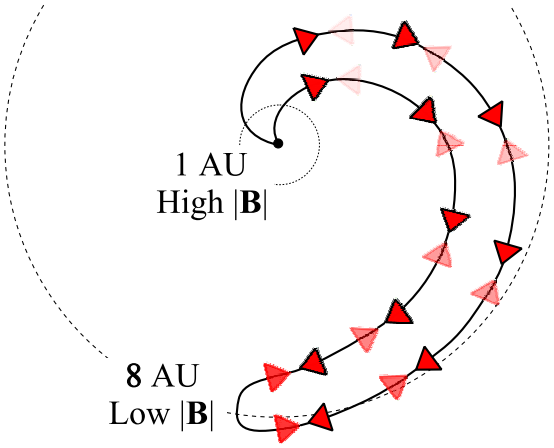

Figure 6. An illustration of the effect of solar rotation on the magnetic field line (black lines) length of ICMEs. When the leading edge of an ICME is at 8 AU, suprathermal electrons (red arrows) must travel ~40 AU to provide the counterstreaming signature at 1 AU. Note also that outward streaming electrons (black outline) are adiabatically focused by moving into weaker magnetic fields, whereas the inward streaming electrons (no outline) are defocused by traveling into stronger fields.

[42] Assuming the counterstreaming electron beam at 1 AU fades when the ICME leading edge is at 6–8 AU, the simulation with LASCO-observed CME times predicts the following 1-AU occurrence rates: CSEs are expected to be observed ~5% of the time at solar minimum, rising to ~25–30% of the time at solar maximum. These numbers are slightly higher than those reported by *Gosling et al.* [1992] for the previous solar cycle but in agreement with those reported by *Skoug et al.* [2000] for the modeled solar cycle. EDs are expected to be rare throughout the solar cycle, varying from $\leq$1% at solar minimum to ~5% at solar maximum. Although ED occurrence rates are difficult to determine, the HFD rate of 6% during the rising phase of solar cycle 23 minus the ~1% rate of those HFDs that are clearly cases of pitch angle scattering gives ~5% as an upper limit [*Pagel et al.*, 2005]. Further analysis is underway to provide a more accurate estimate of the ED occurrence rate.

[43] This prediction of negligible ED occurrence rates compared to CSE rates at 1 AU is one of the most important findings of the model. These contrast with the expectations of *McComas et al.* [1992]. They estimated that during the 18 months leading to the maximum of solar cycle 22, the amount of closed flux introduced by CMEs was four times the amount of disconnected flux created elsewhere, based upon HFD observations, and implied that these should be the same to achieve flux balance. In our models, the amount of closed flux introduced by CMEs is fully balanced by the amount of flux that interchange reconnects or disconnects to produce EDs, as it must be; but the long timescale over which the balancing process occurs compared to the 1-AU

distance of the observing point from the Sun makes a considerable difference in CSE and ED occurrence rates there. EDs can only be observed when the inverted/disconnected fields that carry them lie sunward of 1 AU, whereas CSEs continue to be observed when the leading edges of the loops that carry them lie well beyond 1 AU.

[44] In view of the fact that ultimately all magnetic field lines close somewhere, one might argue that the two scenarios modeled here, one with interchange reconnection opening ICME fields and the other with disconnection elsewhere, could be construed as the same process. An advantage of the former, in addition to providing a possible mechanism for the heliospheric polarity reversal over the solar cycle [*Owens et al.*, 2007] is that open flux is conserved, while the latter requires some unspecified mechanism for balancing the closed flux in ICMEs with the same amount of disconnected flux elsewhere. Once fields have passed far out into the heliosphere, however, keeping track of whether reconnection at the Sun is occurring between the leg of a loop and an open field or between two open fields seems unimportant, since all of the field lines, if followed out far enough, are loops. What is important is that the flux from CMEs does not continue to build, and either interchange reconnection or disconnection can prevent that buildup.

[45] In conclusion, we have proposed that the suprathermal electron signature of the interchange reconnection that opens ICME field-line loops long after their leading edges have passed beyond 1 AU is identical to the signature of disconnection, i.e., a dropout of the electron flux. We have used an analytical model to calculate its occurrence rate at 1 AU, under the assumption that all closed ICME fields eventually open, and find that it should be far less than the occurrence rate of the closed-field signature, in general agreement with observations. The same result holds under the alternative, earlier assumption that closed ICME flux is balanced by true disconnection elsewhere.

[46] **Acknowledgments.** This research was supported by the National Science Foundation Agreement ATM-012950, which funds the CISM project of the STC program, with additional support from NSF grant ATM-0553397.

[47] Amitava Bhattacharjee thanks Adam Rees and Peter Kiraly for their assistance in evaluating this paper.

References

Crooker, N. U., J. Gosling, and T. S. W. Kahler (2002), Reducing heliospheric flux from coronal mass ejections without disconnection, *J. Geophys. Res.*, *107*, (A2), 1028, doi:10.1029/2001JA000236.

Crooker, N. U., R. Forsyth, A. Rees, J. T. Gosling, and S. W. Kahler (2004), Counterstreaming electrons in magnetic clouds near 5 AU, *J. Geophys. Res.*, *109*, A06110, doi:10.1029/2004JA010426.

Gosling, J. T., D. N. Baker, S. J. Bame, W. C. Feldman, and R. D. Zwickl (1987), Bidirectional solar wind electron heat flux events, *J. Geophys. Res.*, *92*, 8519–8535.

Gosling, J. T., D. J. McComas, J. L. Phillips, and S. J. Bame (1992), Counterstreaming solar wind halo electron events—Solar cycle variations, *J. Geophys. Res.*, *97*, 6531–6535.

Gosling, J. T., J. Birn, and M. Hesse (1995), Three-dimensional magnetic reconnection and the magnetic topology of coronal mass ejection events, *Geophys. Res. Lett.*, *103*, 1941–1954.

Hammond, C. M., W. C. Feldman, D. J. McComas, J. L. Phillips, and R. J. Forsyth (1996), Variation of electron-strahl width in the high-speed solar wind: ULYSSES observations, *Astron. Astrophys.*, *316*, 350–354.

Lockwood, M., R. J. Forsyth, A. Balogh, and D. J. McComas (2004), Open solar flux estimates from near-Earth measurements of the interplanetary magnetic field: Comparison of the first two perihelion passes of the Ulysses spacecraft, *Ann. Geophys.*, *22*, 1395–1405Sref-ID:1432-0576/ag/2004-22-1395.

McComas, D. J., J. T. Gosling, J. L. Phillips, S. J. Bame, J. G. Luhmann, and E. J. Smith (1989), Electron heat flux dropouts in the solar wind: Evidence for interplanetary magnetic field reconnection?, *J. Geophys. Res.*, *94*, 6907–6916.

McComas, D. J., J. T. Gosling, and J. L. Phillips (1992), Interplanetary magnetic flux: Measurement and balance, *J. Geophys. Res.*, *97*, 171–177.

Maksimovic, M., et al. (2005), Radial evolution of the electron distribution functions in the fast solar wind between 0.3 and 1.5 AU, *J. Geophys. Res.*, *110*, A09104, doi:10.1029/2005JA011119.

Owens, M. J., and N. U. Crooker (2006), Coronal mass ejections and magnetic flux buildup in the heliosphere, *J. Geophys. Res.*, *111*, A10104, doi:10.1029/2006JA011641.

Owens, M. J., N. A. Schwadron, N. U. Crooker, Spence, W. J. Hughes, and H. E. Spence (2007), Role of coronal mass ejections in the heliospheric Hale cycle, *Geophys. Res. Lett.*, *34*, L06104, doi:10.1029/2006GL028795.

Pagel, C., N. U. Crooker, D. E. Larson, S. W. Kahler, and M. J. Owens (2005), Understanding electron heat flux signatures in the solar wind, *J. Geophys. Res.*, *110*, A01103, doi:10.1029/2004JA010767.

Riley, P., J. T. Gosling, and N. U. Crooker (2004), Ulysses observations of the magnetic connectivity between coronal mass ejections and the Sun, *Astrophys. J.*, *608*, 1100–1105.

Skoug, R. M., W. C. Feldman, J. T. Gosling, D. J. McComas, and C. W. Smith (2000), Solar wind electron characteristics inside and outside coronal mass ejections, *J. Geophys. Res.*, *105*, 23,069–23,084.

Wimmer-Schweingruber, R. F., et al. (2006), Understanding interplanetary coronal mass ejection signatures, *Space Sci. Rev.*, *123*, 177–216, doi:10.1007/s11214-006-9017-x.

Yashiro, S., N. Gopalswamy, G. Michalek, O. C. St. Cyr, S. P. Plunkett, N. B. Rich, and R. A. Howard (2004), A catalog of white light coronal mass ejections observed by the SOHO spacecraft, *J. Geophys. Res.*, *109*, A07105, doi:10.1029/2003JA010282.

N. U. Crooker and M. J. Owens, Center for Space Physics, Boston University, Boston, MA 02215, USA. (mjowens@bu.edu)